ESTIMATION OF SPECTRAL LINES USING EXPECTATION PROPAGATION

Jiang Zhu[‡] *Xupeng Lei*[‡] *Mihai-Alin Badiu*[†]

[‡] Ocean College, Zhejiang University, Zhoushan, 316021, China
[†] Department of Engineering Science, University of Oxford, Oxford, OX13PJ, England

ABSTRACT

We consider the line spectral estimation (LSE) from general linear/nonlinear measurements obtained through a generalized linear model (GLM). This paper develops expectation propagation (EP) based LSE (EPLSE) method. The proposed method automatically estimates the model order, noise variance, and can deal with the nonlinear measurements. Numerical experiments show the excellent performance of EPLSE.

Index Terms— LSE, expectation propagation, compressed sensing, nonlinear measurements

1. INTRODUCTION

Line spectral estimation aiming to extract the frequencies of a mixture of sinusoids is a fundamental problem in signal processing fields due to its wide application arising in sonar, communication and radar fields [1]. Classical methods include maximum likelihood (ML) [2] and subspace methods such as multiple signal classification (MUSIC) and estimation of signal parameters via rotational invariant techniques (ESPRIT) [3]. The ML approach maximizes a nonconvex function which has a multimodal shape with a sharp global maximum, which requires accurate initialization. Compared to subspace based approaches, ML performs better when the samples is limited or the SNR is small.

Compressed sensing (CS) based approaches which exploit the sparsity of the signal are proposed. By discretizing the frequency into a number of grids to construct a dictionary matrix, the original nonlinear frequency estimation problem is transformed to be a sparse linear inverse problem [4]. Since the frequency is continuous-valued, discretization incurs grid mismatch [5]. As a result, off-grid methods are proposed, which refine the grid gradually to overcome the grid mismatch effectively [6–8].

To work directly with continuously parameterized dictionaries, gridless methods are proposed and can be classified into two categories: atomic norm based [9–11] and variational LSE (VALSE) [12] approaches. The atomic norm based approaches allow for working with an infinite, continuous dictionary and are proved to recover the well separated frequencies perfectly in the noiseless case. While for the VALSE, it treats the frequency as random variables, and it automatically estimates the model order, the noise variance and the posterior probability density functions (PDF) of the frequencies. As for the computation complexity, the atomic norm based approaches involve solving a semidefinite programming (SDP), which is usually very high. In contrast, VALSE is implemented with much lower computation complexity, but performing the LSE sequentially.

From the Bayesian algorithm point of view, approximate message passing (AMP) [13] and generalized approximate message passing (GAMP) [14] are proposed to deal with the sparse signal recovery from linear and nonlinear measurements. It is shown that both AMP and GAMP can be derived from expectation propagation (EP) [15–19].By treating the frequency and amplitudes as random variables and formalize the factor graph, we derive EP based LSE (EPLSE). We adopt the Bernoulli Gaussian prior distribution to estimate the model order. In addition, expectation maximization (EM) is incorporated to iteratively learn both the parameters of the prior and output distribution [20].

2. PROBLEM SETUP

Let $\mathbf{z} \in \mathbb{C}^M$ be a line spectrum signal consisting of K complex sinusoids

$$\mathbf{z} = \sum_{k=1}^{K} \mathbf{a}(\theta_k) x_k, \tag{1}$$

where x_k is the complex amplitude of the kth frequency, $\theta_k \in [-\pi, \pi)$ is the kth frequency, and

$$\mathbf{a}(\theta) = [1, \mathrm{e}^{\mathrm{j}\theta}, \cdots, \mathrm{e}^{\mathrm{j}(M-1)\theta}]^{\mathrm{T}}. \tag{2}$$

The LSE undergoes a componentwise (linear or nonlinear) transform, which is described as a conditional PDF $p(\mathbf{y}|\mathbf{z};\boldsymbol{\omega}_z)$

$$p(\mathbf{y}|\mathbf{z};\boldsymbol{\omega}_z) = \prod_{m=1}^{M} p(y_m|z_m;\boldsymbol{\omega}_z), \tag{3}$$

where $\boldsymbol{\omega}_z$ are the unknown nuisance parameters. In the following text, we illustrate some examples about $p(\mathbf{y}|\mathbf{z})$.

This work is supported by NSFC under Grants 62371420 and 61901415 and Zhejiang Provincial Natural Science Foundation of China under Grant LY22F010009.

- The Line spectral signal is corrupted by the additive white Gaussian noise and is described by

$$\mathbf{y} = \mathbf{z} + \mathbf{w}, \tag{4}$$

where $\mathbf{w} \sim \mathcal{CN}(\mathbf{w}; \mathbf{0}, \sigma^2 \mathbf{I}_M)$, σ^2 is the variance of the noise.

- Quantized measurements: $\mathbf{y} = Q(\mathbf{z} + \mathbf{w})$, where $Q(\cdot)$ denotes a quantizer which maps the continuous values into discrete numbers.

For all the listed cases, $\boldsymbol{\omega}_z$ refers to the variance of the noise.

Since the sparsity level K is usually unknown, the line spectrum signal consisting of N complex sinusoids is assumed [12]

$$\mathbf{z} = \sum_{n=1}^{N} x_n \mathbf{a}(\theta_n) \triangleq \mathbf{A}(\boldsymbol{\theta})\mathbf{x}, \tag{5}$$

where $\mathbf{A}(\boldsymbol{\theta}) = [\mathbf{a}(\theta_1), \cdots, \mathbf{a}(\theta_N)]$ and $N \leq M$. For the complex coefficients, i.i.d. distribution is used, i.e.,

$$p(\boldsymbol{\theta}) = \prod_{n=1}^{N} p(\theta_n), \quad p(\mathbf{x}; \boldsymbol{\omega}_x) = \prod_{n=1}^{N} p(x_n; \boldsymbol{\omega}_x), \tag{6}$$

where

$$p(x_n; \boldsymbol{\omega}_x) = (1 - \pi_n)\delta(x_n) + \pi_n \mathcal{CN}(x_n; \mu_0, \tau_0), \tag{7}$$

$\boldsymbol{\omega}_x = [\pi_1, \cdots, \pi_N, \mu_0, \tau_0]^{\mathrm{T}}$ are unknown parameters. Note that Bernoulli Gaussian distribution can be imposed to enforce sparsity. For the prior distribution $p(\theta_n)$, von Mises distribution can be encoded. For uninformative prior, we assume $p(\theta_n) = 1/(2\pi)$, $\forall\ n$. Directly solving the ML estimate of $\{\boldsymbol{\omega}_x, \boldsymbol{\omega}_z\}$ or the MMSE estimate of $\{\boldsymbol{\theta}, \mathbf{x}\}$ are both intractable. As a result, an iterative algorithm is designed.

3. EPLSE ALGORITHM

The factor graph is presented in Fig. 1 and a delta factor node $\delta(\cdot)$ is introduced. Before derivation, the following notations in Table 1 are used. First, we initialize $m_{\delta \to z}(\mathbf{z}) = \mathcal{CN}(\mathbf{z}, \mathbf{z}_{\mathrm{A}}^{\mathrm{ext}}, \mathrm{diag}(\mathbf{v}_{\mathrm{A}}^{\mathrm{ext}}))$, $m_{n \to m}(x_n) \triangleq \mathcal{CN}(x_n; x_{n \to m}, \sigma^2_{n \to m})$ and $m_{n \to m}(\theta_n) \triangleq \mathcal{VM}(\theta_n; \mu_{n \to m}, \kappa_{n \to m})$. Then we briefly present the details on how to update the messages to perform line spectral estimation in Algorithm 1. For further details, please refer to [21].

4. NUMERICAL SIMULATION

In this section, the performance of EPLSE is evaluated by performing numerical simulations. In addition, EPLSE is compared with VALSE [12] under different scenarios.

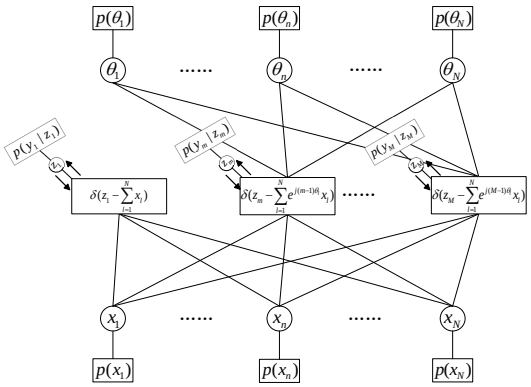

Fig. 1: The whole factor graph. Here we introduce a delta factor node $\delta(\cdot)$, which simplifies the calculation as shown later .

Algorithm 1 EPLSE algorithm

Initialize $x_{k \to m}$ and $\sigma^2_{n \to m}$, $\mu_{n \to m}$, $\kappa_{k \to m}$, $\mathbf{z}_{\mathrm{A}}^{\mathrm{ext}}$, $\mathbf{v}_{\mathrm{A}}^{\mathrm{ext}}$. Set the number of outer iterations T_{o} and the threshold $\gamma = 0.5$ to determine the model order;
for $t_{\mathrm{outer}} = 1, \cdots, T_{\mathrm{outer}}$ **do**
  Update $m_{z \to \delta}(\mathbf{z})$.
  for $t_{\mathrm{inner}} = 1, \cdots, T_{\mathrm{inner}}$ **do**
    Compute $\tilde{m}_{m \to n}(\theta_n)$.
    Update $m_{n \to m}(\theta_n)$.
    Compute $\tilde{m}_{m \to n}(x_n)$.
    Update $m_{n \to m}(x_n)$.
  end for
  Compute $m_{\delta \to z}$.
end for
Return $\hat{\theta}_n$, $\hat{x}_k$, and $\hat{K} = \sum_{n=1}^{N} 1\{\pi_n^{\mathrm{new}} > \gamma\}$.

Simulation Setup: The simulation is almost the same as [12]. For completeness, we present the details. The frequencies $\{\tilde{\theta}\}_{k=1}^{K}$ is drawn from $\mathcal{U}(-\pi, \pi)$ and the minimum wrap-around distance $\Delta\theta$ of the frequencies is $\Delta\theta = 2\pi/N$. The complex coefficients $\{\tilde{x}\}_{k=1}^{K}$ are generated by drawing their magnitudes from $\mathcal{N}(1, 0.2)$ and phases from $\mathcal{U}(-\pi, \pi)$. For the additive measurement noise model (4), The SNR is defined as $\mathrm{SNR} = 10 \log \frac{\|\mathbf{z}\|_2^2}{\mathrm{E}\|\mathbf{w}\|_2^2} = 10 \log \frac{\|\mathbf{z}\|_2^2}{M\sigma_w^2}$, where σ_w^2 denotes the variance of the additive noise $\mathbf{w}$. For both the EPLSE and VALSE algorithm, no prior information about the frequencies is assumed, and we set $p(\theta_n) = 1/(2\pi),\ n = 1, \cdots, N$. Both EPLSE and VALSE stop at iteration t if $\|\hat{\mathbf{z}}(t) - \hat{\mathbf{z}}(t-1)\| / \|\hat{\mathbf{z}}(t)\| < 10^{-6}$ or the number of iterations reaches 2000. For the assumed number of sinusoids N, we set $N = M$.

Three performance metrics are used:

- The normalized mean squared error of signal reconstruction: $20 \log \frac{\|\hat{\mathbf{z}} - \mathbf{z}\|_2}{\|\mathbf{z}\|_2}$,

Table 1: Notations used for derivation

$\tilde{m}_{\delta\to z_m}(z_m) \triangleq \mathcal{CN}(z_m; z_{\mathrm{A},m}^{\mathrm{ext}}, v_{\mathrm{A},m}^{\mathrm{ext}})$	The message from the factor node $\delta\left(z_m - \sum_{l=1}^{N} \mathrm{e}^{\mathrm{j}(m-1)\theta_l} x_l\right)$ to the variable node z_m
$m_{z_m\to\delta}(z_m) \triangleq \mathcal{CN}(z_m; z_{\mathrm{B},m}^{\mathrm{ext}}, v_{\mathrm{B},m}^{\mathrm{ext}})$	The message from the variable node z_m to the factor node $\delta\left(z_m - \sum_{l=1}^{N} \mathrm{e}^{\mathrm{j}(m-1)\theta_l} x_l\right)$
$\tilde{m}_{m\to n}(\theta_n) \triangleq \mathcal{VM}(\theta_n; \tilde{\mu}_{m\to n}, \tilde{\kappa}_{m\to n})$	The message from the factor node $\delta\left(z_m - \sum_{l=1}^{N} \mathrm{e}^{\mathrm{j}(m-1)\theta_l} x_l\right)$ to the variable node θ_n
$\tilde{m}_{m\to n}(x_n) \triangleq \mathcal{CN}(x_n; \tilde{x}_{m\to n}, \tilde{\sigma}_{m\to n}^2)$	The message from the factor node $\delta\left(z_m - \sum_{l=1}^{N} \mathrm{e}^{\mathrm{j}(m-1)\theta_l} x_l\right)$ to the variable node x_n
$m_{n\to m}(\theta_n) \triangleq \mathcal{VM}(\theta_n; \mu_{n\to m}, \kappa_{n\to m})$	The message from the variable node θ_n to the factor node $\delta\left(z_m - \sum_{l=1}^{N} \mathrm{e}^{\mathrm{j}(m-1)\theta_l} x_l\right)$
$m_{n\to m}(x_n) \triangleq \mathcal{CN}(x_n; x_{n\to m}, \sigma_{n\to m}^2)$	The message from the variable node x_n to the factor node $\delta\left(z_m - \sum_{l=1}^{N} \mathrm{e}^{\mathrm{j}(m-1)\theta_l} x_l\right)$

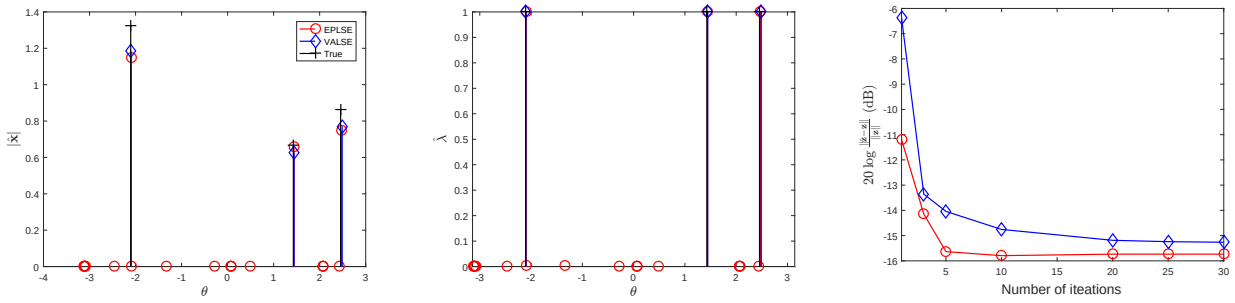

(a) (b) (c)

Fig. 2: A single realization of the performance of EPLSE. Fig. 2(a), Fig. 2(b) and Fig. 2(c) correspond to the amplitude reconstruction $\hat{\mathbf{x}}$, the sparsity $\boldsymbol{\lambda}$, signal reconstruction error, respectively.

- The empirical probability of successfully estimating the model order $\Pr(\hat{K} = K)$.
- The frequency estimation error $20\log\|\hat{\boldsymbol{\theta}} - \boldsymbol{\theta}\|_2$ (dB) averaged over the trials in which the model order is estimated correctly.

At first, a simple simulation is conducted to show the recovery results of EPLSE. We set $M = 21$, $|\mathcal{M}| = 18$ which corresponds to the incomplete data case, $K = 3$, and the true frequencies and complex coefficients are $\boldsymbol{\theta} = [-2.1050, 1.4278, 2.4550]^{\mathrm{T}}$ and $\mathbf{x} = [1.3154 + 0.1524\mathrm{j}, 0.6064 - 0.2788\mathrm{j}, 0.6544 - 0.5616\mathrm{j}]^{\mathrm{T}}$, respectively. The SNR is set as 10 dB. The results are shown in Fig. 2. It can be seen that EPLSE performs well and the model order is estimated correctly.

4.1. Performance with Number of Measurements

The performance versus the number of measurements are investigated. The number of spectral is $K = 3$ and $\mathrm{SNR} = 20$ dB. Results are shown in Fig. 3. It can be seen that the signal reconstruction and frequency estimation error of EPLSE is higher than that of VALSE. As for the model order probability, EPLSE is higher than VALSE.

4.2. Performance with Number of Spectra

We investigate the performance of EPLSE when the number of spectral K is varied. We set $M = 21, \mathrm{SNR} = 20$ dB. It can be seen that EPLSE achieves almost the same performance as VALSE in terms of signal reconstruction and frequency estimation error. As for the model order estimation probability, EPLSE performs better.

4.3. Estimation from Nonlinear (Quantized) Measurements

Here we illustrate the performance of Gr-EPLSE through low precision quantized measurements. We set $N = M = 41$ and $K = 3$. The results are shown in Fig. 5. For one-bit quantization, zero threshold is chosen and the amplitude information is lost in noiseless setting, thus the debiased NMSE (dNMSE) $\min_{c\in\mathbb{C}} 20\frac{\|c\hat{\mathbf{z}}-\mathbf{z}\|_2}{\|\mathbf{z}\|_2}$ is used instead. For multi-bit quantization, a

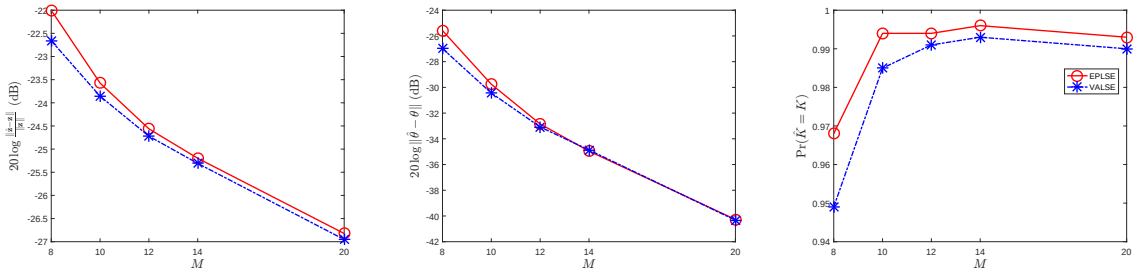

(a) (b) (c)

Fig. 3: Results versus M averaged over 1000 MC trials. Fig. 3(a), Fig. 3(b) and Fig. 3(c) correspond to the signal reconstruction error, frequency estimation error and model order recovery probability, respectively.

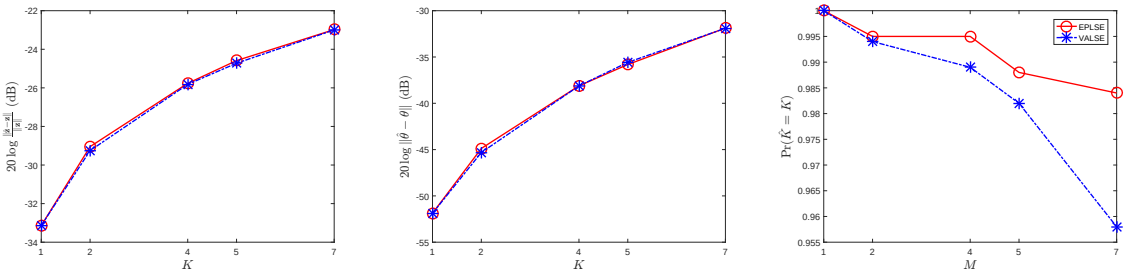

(a) (b) (c)

Fig. 4: Results versus K averaged over 1000 MC trials. Fig. 4(a), Fig. 4(b) and Fig. 4(c) correspond to the signal reconstruction error, frequency estimation error and model order recovery probability, respectively.

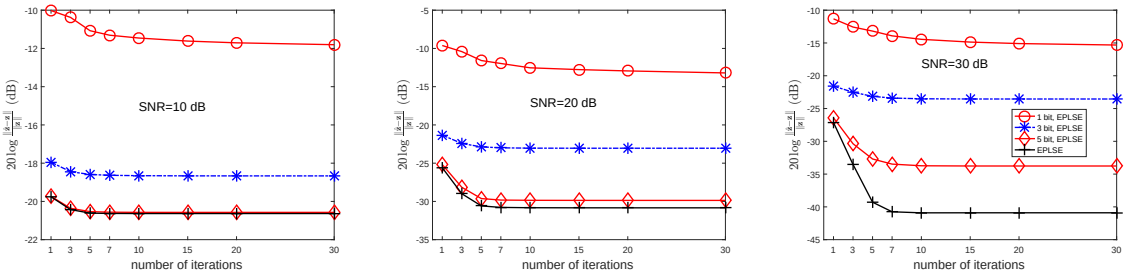

(a) (b) (c)

Fig. 5: The NMSE versus iteration averaged over 20 MC trials. Fig. 5(a), Fig. 5(b) and Fig. 5(c) correspond to the SNR 10 dB, 20 dB and 30 dB, respectively.

uniform quantizer is chosen. The real and imaginary parts of the measurements are quantized separately, and the dynamic range of the quantizer is restricted to be $[-3\sigma_z/\sqrt{2}, 3\sigma_z/\sqrt{2}]$, where σ_z^2 is the variance of $\mathbf{z}$. In our setting we have $\sigma_z^2 \approx K$. For 1 bit quantization, we input the noise variance to be 1 and for multi-bit quantization, EM is used to iteratively estimate the noise variance. Results are shown in Fig. 5. It can be seen that EPLSE converges, and the performance improves as bit depth or SNR increases.

5. CONCLUSION

This paper proposes EPLSE algorithm for LSE. By incorporating the Bernoulli Gaussian distribution for sparsity and EM algorithm, EPLSE automatically estimates the model order, noise variance. In addition, EPLSE provides the posterior PDF of the frequencies, which is beneficial for sequential estimation. Numerical results demonstrate the excellent performance of EPLSE.

6. REFERENCES

[1] P. Stoica and R. L. Moses, *Spectral Analysis of Signals.* Upper Saddle River, NJ, USA: Prentice-Hall, 2005.

[2] P. Stoica and A. Nehorai, "Music, maximum likelihood and Cramér-Rao bound: further results and comparisons," *IEEE Trans. Acoust., Speech, Signal Processing*, vol. 38, no. 12, pp. 2140-2150, Dec. 1990.

[3] B. Ottersten, M. Viberg and T. Kailath, "Analysis of subspace fitting and ML techniques for parameter estimation from sensor array data," *IEEE Trans. Signal Process.*, vol. 40, pp. 590-600, Mar. 1992.

[4] D. Malioutov, M. Cetin and A. Willsky, "A sparse signal reconstruction perspective for source localization with sensor arrays," *IEEE Trans. Signal Process.*, vol. 53, no. 8, pp. 3010-2022, 2005.

[5] Y. Chi, L. L. Scharf, A. Pezeshki, and R. Calderbank, "Sensitivity to basis mismatch in compressed sensing," *IEEE Trans. Signal Process.*, vol. 59, no. 5, pp. 2182-2195, 2011.

[6] L. Hu, Z. Shi, J. Zhou and Q. Fu, "Compressed sensing of complex sinusoids: An approach based on dictionary refinement" *IEEE Trans. Signal Process.*, vol. 60, no. 7, pp. 3809-3822, 2012.

[7] L. Hu, J. Zhou, Z. Shi, Q. Fu, "A fast and accurate reconstruction algorithm for compressed sensing of complex sinusoids," *IEEE Trans. Signal Process.*, vol. 61, no. 22, pp. 5744-5754, 2013.

[8] J. Fang, F. Wang, Y. Shen, H. Li and R. S. Blum, "Super-resolution compressed sensing for line spectral estimation: an iterative reweighted approach," *IEEE Trans. Signal Process.*, vol. 64, no. 18, pp. 4649-4662, 2016.

[9] V. Chandrasekaran, B. Recht, P. A. Parrilo, and A. S. Willsky, "The convex geometry of linear inverse problems," *Foundations of Computational Mathematics*, vol. 12, no. 6, pp. 805-849, 2012.

[10] Z. Yang, L. Xie and C. Zhang, "A discretization-free sparse and parametric approach for linear array signal processing," *IEEE Trans. Signal Process.*, vol. 62, no. 19, pp. 4959-4973, 2014.

[11] Z. Yang and L. Xie, "On gridless sparse methods for line spectral estimation from complete and incomplete data," *IEEE Trans. Signal Process.*, vol. 63, no. 12, pp. 3139-3153, 2015.

[12] M. A. Badiu, T. L. Hansen and B. H. Fleury, "Variational Bayesian inference of line spectral," *IEEE Trans. Signal Process.*, vol. 65, no. 9, pp. 2247-2261, 2017.

[13] D. L. Donoho, A. Maleki, and A. Montanari, "Message passing algorithms for compressed sensing: I. Motivation and construction" *in Proc. Inf. Theory Workshop*, Cairo, Egypt, Jan. 2010, pp. 1-5.

[14] S. Rangan, "Generalized approximate message passing for estimation with random linear mixing," *in Proc. IEEE Int. Symp. Inf. Theory*, Jul. 2011, pp. 2168-2172.

[15] X. Meng, S. Wu, L. Kuang, and J. Lu, "An expectation propagation perspective on approximate message passing," *IEEE Signal Process. Lett.*, vol. 22, no. 8, pp. 1194-1197, Aug. 2015.

[16] S. Wu, L. Kuang, Z. Ni, J. Lu, D. Huang, and Q. Guo, "Low-complexity iterative detection for large-scale multiuser MIMO-OFDM systems using approximate message passing," *IEEE J. Sel. Topics Signal Process.*, vol. 8, no. 5, pp. 902-915, May 2014.

[17] X. Meng, S. Wu and J. Zhu, "A unified Bayesian inference framework for generalized linear models," *IEEE Signal Process. Lett.*, vol. 25, no. 3, pp. 398-402, 2018.

[18] J. Zhu, "A comment on the "A unified Bayesian inference framework for generalized linear models"," arXiv preprint, 2019.

[19] T. Minka, "A family of algorithms for approximate Bayesian inference," Ph.D. dissertation, Department of Electrical Engineering and Computer Science, Mass. Inst. Technol., Cambridge, MA, USA, 2001.

[20] J. P. Vila and P. Schniter, "Expectation-maximization Gaussian-mixture approximate message passing," *IEEE Trans. Signal Process.*, vol. 61, no. 19, pp. 4658-4672, Oct. 2013.

[21] J. Zhu and M. A. Badiu, "Expectation propagation line spectral estimation," arXiv: 1907.09094.